Journal of Colloid and Interface Science 426 (2014) 31–38

Contents lists available at ScienceDirect

Journal of Colloid and Interface Science

www.elsevier.com/locate/jcis

Gold nanoparticles decorated with oligo(ethylene glycol) thiols: Surface charges and interactions with proteins in solution

Moritz Schollbach [a], Fajun Zhang [a,*], Felix Roosen-Runge [a], Maximilian W.A. Skoda [b], Robert M.J. Jacobs [c], Frank Schreiber [a]

[a] Institut für Angewandte Physik, Universität Tübingen, Auf der Morgenstelle 10, D-72076 Tübingen, Germany
[b] STFC, ISIS, Rutherford Appleton Laboratory, Chilton, Didcot OX11 0OX, United Kingdom
[c] Department of Chemistry, Chemistry Research Laboratory, University of Oxford, Mansfield Road OX1 3TA, United Kingdom

ARTICLE INFO

Article history:
Received 13 February 2014
Accepted 25 March 2014
Available online 3 April 2014

Keywords:
Gold nanoparticles
Oligo(ethylene glycol) thiol
Self-assembled monolayer
DLS
Zeta-potential
UV–visible spectroscopy

ABSTRACT

We have studied oligo(ethylene glycol) (OEG) thiol self-assembled monolayer (SAM) coated gold nanoparticles (AuOEG) and their interactions with proteins in solutions using electrophoretic and dynamic light scattering (ELS and DLS). The results are compared with poly(ethylene glycol) (PEG) thiol coated AuNPs (AuPEG). We show that both AuOEG and AuPEG particles carry a low net negative charge and are very stable (remaining so for more than one year), but long-term aging or dialysis can reduce the stability. If the decorated AuNPs are mixed with bovine serum albumin (BSA), both effective size and zeta-potential of the AuNPs remain unchanged, indicating no adsorption of BSA to the colloid surface. However, when mixed with lysozyme, zeta-potential values increase with protein concentrations and lead to a charge inversion, indicating adsorption of lysozyme to the colloid surface. The colloidal solutions of AuOEG become unstable near zero charge, indicated by a cluster peak in the DLS measurements. The AuPEG solutions show similar charge inversion upon addition of lysozyme, but the solutions are stable under all experimental conditions, presumably because of the strong steric effect of PEG. Washing the protein bound colloids by centrifugation can remove only part of the adsorbed lysozyme molecules indicating that a few proteins adsorb strongly to the colloids. The effective charge inversion and rather strongly bound lysozyme on the colloid surface may suggest that in addition to the charges formed at the SAM–water interface, there are defects on the surface of the colloid, which are accessible to the proteins. The results of this study of surface charge, and stability shed light on the interaction with proteins of SAM coated AuNPs and their applications.

1. Introduction

Monolayer-protected colloidal gold has many unusual properties which have been widely used for biodiagnostics, bio- and chemical sensors, drug delivery and biomolecular recognition purposes [1–4]. Gold nanoparticles (AuNP) decorated by poly(ethylene glycol) (PEG) and oligo(ethylene glycol) (OEG) thiol self-assembled monolayer (SAM) have potential applications in bio-nanotechnology due to their unique property of preventing the non-specific absorption of protein on the colloidal surface as well as bacterial adhesion [5]. Whereas resistance to protein adsorption by PEG can be theoretically explained by the unfavorable free-energy change caused by dehydration and steric confinement of the long polymer [6,7], a complete picture concerning the mechanism of protein resistance of OEG SAMs has still not fully been obtained. Experiments have suggested that the tightly bound water layer at the interface could form a physical barrier to prevent direct contact between the protein and the interface [8–10]. Recent results in our group indicate a rather strong interaction of OEG SAMs with water and the penetration of water into the SAM [11–15]. Feldman et al. have reported an electrostatic, long-ranged repulsive interaction with fibrinogen functionalized AFM tips upon approaching to OEG grafted gold substrates [16]. This repulsive potential is thought to arise from a tightly bound layer of hydroxide ions, which preferably penetrate into the SAM and create a net negative electrostatic potential, which then acts against the also negatively charged protein molecules [17]. Further studies using chemical force spectroscopy on the direct interactions between a hydrophobic probe and OEG SAMs at various pH values and with several

* Corresponding author. Fax: +49 7071 295110.
E-mail address: fajun.zhang@uni-tuebingen.de (F. Zhang).

http://dx.doi.org/10.1016/j.jcis.2014.03.052
0021-9797/

different added salts indicate that not only the bound water but also electrostatics has an effect on the interactions [16–23]. Studies by Kreuzer and Pertsin suggest that the charge at the SAM–water interface is due to the preferential adsorption of the hydroxide ions ($OH-$) over hydronium (H_3O+) from the aqueous solution, which explains the measured negative surface charges [21,23].

Despite the importance of these issues, there have been only a few studies involving OEG SAM coated AuNPs. Zheng and Huang have synthesized ethylene glycol (EG) monolayer coated AuNPs with a mean size of 3.0–3.5 nm [24,25]. The resulting functionalized AuNPs are very stable even at high ionic strength and allow re-dispersion after centrifugation and drying. Protein binding measurements using gel-electrophoresis and ion-exchange chromatography with several proteins of different isoelectric point and hydrophobicity (BSA, lysozyme, cytochrome C, ribonuclease A and myoglobin) indicate no detectable binding of proteins to the OEG coated AuNPs [24,25]. AuNPs protected by mixed monolayers allow the design of specific interactions with target molecules [26]. For this purpose, a biotin group or glutathione has been capped onto the surface of AuNPs protected by tri(ethylene glycol) thiols. Specific binding of streptavidin and glutathione-*S*-transferase to their respective capped AuNPs is observed [26]. On the other hand, it is known that directly synthesized alkanethiol-protected gold colloids are limited to a size of 1–10 nm which limits their application [27–30]. The post-decoration method by replacing the citrate stabilized AuNPs with thiols has no such limit and we have been successful in decoration up to 40 nm AuNPs with EG6OH [31]. Because of van der Waals adhesion or binding energies increasing with the size of particles [32], short chain OEG thiols with 2–4 EG units can stabilize only small AuNPs (<3 nm) in solution. For larger AuNPs (>10 nm), OEG thiols below six EG units cannot stabilize the colloids. In our previous work, although difficult, we have been successful in decorating AuNPs up to 40 nm in diameter with EG6OH [31].

We have further established a method based on the depletion effect in a mixture to characterize the interactions between OEG SAM coated AuNPs with proteins in solution [31,33,34]. Experimental observations suggest that these functionalized AuNPs exhibit protein resistance, and that the resulting repulsion combined with the depletion effect make it easy to see aggregation *via* the color change of AuNP solutions. The mixture of the protein and functionalized AuNPs is very sensitive to the nature of the added salt. Following the Hofmeister series, salting-in salts enhance the stability of the mixture and salting-out salts reduce it [34]. This depletion-driven colloid aggregation requires a high protein volume fraction (>10% depending on the size ratio between colloid and protein). However, the exact interactions between protein and colloid at the interface, the status of the surface charge of the colloid and its effect on the interaction is still not clear.

In this work, we present a systematic characterization of the surface charge of OEG SAM coated AuNPs, their stability and interactions with proteins in solution. We aim to address the following questions: firstly, what is the state of the surface charge on the SAM coated AuNPs and what are the control parameters? Secondly, what is the effect of the surface charge on the interactions with proteins in solutions as well as the long-term stability, and whether the charge state of proteins, i.e. the acidic or basic nature of the protein, also affects the interactions? Thirdly, what is the difference between OEG and PEG SAM coated AuNPs regarding their charge state and interactions with proteins? As a related issue, we address potential differences in the properties of self-assembled monolayers (SAMs) based on the curvature of the underlying surface, as discussed for instance in Ref. [2]. SAM properties must differ on some level because on a curved surface the density of SAM head-groups is always smaller than that of the surface-attachment sites. This density difference increases with increasing curvature and is most pronounced for SAMs formed on nanoscopic particles which can be used as building blocks for special purpose [35,36].

2. Experimental section

2.1. Materials

Citrate-stabilized gold colloids in aqueous solution with mean size of approximately 10 and 20 nm were purchased from British BioCell International (BBI) and were used as received. Hexa (ethylene glycol) terminated thiol, $HS(CH_2)_{11}(OCH_2CH_2)_6OMe$, and $HS(CH_2)_{11}(OCH_2CH_2)_6OH$ abbreviated as EG6OMe and EG6OH, respectively, were purchased from ProChimia, Poland, and were used as received. Poly(ethylene glycol) thiol with molecular weight of 5 kDa (PEG5k) was purchased from Sigma-Aldrich and used as received. Bovine serum albumin (BSA) and lysozyme (LYZ) from chicken egg white were purchased from Sigma-Aldrich.

2.2. Preparation of surface-modified gold colloids

The colloidal gold was modified by directly mixing 1 mL stock solution of thiols (~2 mg/mL) (EG6OH or EG6OMe) to the colloid solution (10 mL) with gentle stirring. This corresponds to an excess of EG6OMe by a factor of between 10^2 and 10^3, based on a simple calculation considering the total surface area of gold colloids and the area occupied by a thiol molecule. The colloid solutions were incubated at 4 °C in a fridge over night. The stability of the modified colloids was examined by monitoring the UV–visible spectra and it was found to be stable in a wide range of temperature (5–70 °C), pH (1.3–12.4), and ionic strength (NaCl, 0–4.0 M). The colloidal solution was further concentrated (approximately by a factor of 10) by using a rotation-evaporation instrument at ~10 mbar at 40 °C for approximately 50 min. Details of this method have been described in previous publications [31,33].

PEG5k coated AuNPs were prepared by following the procedure described in the literature [37]. PEG thiol solution of 0.1 mg/mL was mixed directly with the colloidal solution in the same volume (5 mL each). The mixture was stirred at room temperature overnight. The stability was tested by adding NaCl 1.0 M. No color change was observed. The decorated colloidal solution was further concentrated by centrifugation, i.e. 1 mL solution was filled into sample-tubes, centrifuged for 15 min at 13000 rpm. After that, 0.9 mL of the supernatant was removed and the pellet of colloid was re-dispersed in the remaining solution by vortex mixing. Note that this procedure is not suitable for OEG coated AuNPs, since the pellet cannot be easily re-dispersed.

The protein-colloid mixtures were prepared by addition of a protein stock solution (10 mg/mL or 0.7 μM for lysozyme, 20 mg/ml or 0.3 μM for BSA) to the colloid solution. The resulting samples had a final protein concentration between 0 and 10 mg/mL, as given in the description of the results. We chose a protein concentration which was high enough to cover the colloid surface in case of adsorption, but low enough so as to minimize the impact on the bulk characteristics. The colloid concentration was about two thirds of the original solution as determined from the absorption around 525 nm. This is about 4.7×10^{11} particles/mL (0.8 nM) as the original number density of AuNPs is about 7×10^{11} particles/mL [31]. Selected sample solutions were further treated with a washing procedure: The sample solution was first centrifuged for 10 min at 13,000 rpm and three quarters of the supernatant were then replaced with water. Subsequently, the pellet colloid was re-dispersed by vortex mixing. The size and zeta potential of the re-dispersed colloid solution was determined by dynamic and electrophoretic light scattering. This procedure was repeated several times.

2.3. Methods

2.3.1. Electrophoretic and dynamic light scattering (ELS and DLS)

Size and zeta potential measurements were carried out using a Zetasizer Nano (Malvern Instruments Ltd., UK) with a 3 mW He–Ne laser at $\lambda = 633$ nm. For dynamic light scattering, the instrument was used in the backscattering configuration with $\theta = 173°$. The photon autocorrelation functions were collected continuously using acquisition times of 30 s per correlation function. Measured autocorrelation functions were converted into the distribution of particle size (hydrodynamic diameter, $2R_h$) by using a cumulant [38] and CONTIN analysis [38] provided with the Zetasizer Nano software. Both size and zeta potential measurements were repeated at least 3 times for each sample and the averaged profiles (values) were presented.

In DLS measurements, the diffusion coefficient, D, of the particles is obtained from the autocorrelation function. The particle size is further estimated *via* the Stokes–Einstein equation:

$$D = \frac{k_B T}{6\pi\eta R_h} \tag{1}$$

where D is the diffusion coefficient, η the viscosity of the solvent and the R_h is the hydrodynamic radius of particles. We note that Eq. (1) is of course an approximation in the limit of non-interacting and dilute suspensions of particles. For a discussion of its validity, in particular for solutions of charged proteins, see Ref. [39].

The zeta potential (ζ) was determined using electrophoretic light scattering (ELS) with an alternating electrical field. Sample solutions were filled in a capillary cell (DTS 1060, Malvern Instruments Ltd.). The mobility of particles under an electric field was measured by a frequency shift (Doppler shift) compared to a reference beam at a forward angle ($\theta = 12.8°$), which is related to the zeta potential of the target particles by [40]:

$$\xi = \frac{3\eta\mu E}{2f(\kappa a)\varepsilon} \tag{2}$$

where η is the viscosity of the solvent, μ_E is the electrophoretic mobility of the particles, κ is the inverse Debye length and a is the radius of the particle. Since $\kappa a < 1$ for our conditions, the Henry function $f(\kappa a)$ is set to 1, corresponding to the Hückel–Onsager limit [40]. The ξ-potential measurement was calibrated using a standard solution (DTS 1050, Malvern Instruments Ltd.) with a value of −50 mV. This relation between zeta potential and electrophoretic mobility holds for a non-conducting sphere, although it has been applied successfully also to conducting spheres [41]. The exact relation between zeta potential and electrophoretic mobility depends fundamentally on assumptions on the adsorbed layers of OEG, PEG and protein [42]. The analysis performed in this study is thus not intended to characterize the surface charge in an absolute quantitative way. The derived zeta potentials allow, however, qualitative and relative comparisons and, in particular, a robust monitoring of inversion of the nanoparticle-protein complexes.

2.3.2. UV–visible spectroscopy

UV–visible absorption measurements were performed at room temperature using a Cary 50 UV–visible spectrophotometer (Varian Optical Spectroscopy Instruments). Quartz and disposable PE UV cuvettes with an optical path length through the sample of 1.0 cm were used to contain the sample while collecting the spectra in the wavelength range from 300 to 800 nm.

3. Results and discussion

3.1. OEG and PEG SAM decoration and long term stability

We first show the size and zeta potential measurements of the pure colloid solutions before and after decoration. The results on the stability of such functionalized nanoparticles after long term storage and dialysis against pure water are also presented. For the convenience of description, the EG6OH and EG6OMe decorated AuNPs are denoted as AuxxEG6OH and AuxxEG6OMe, where "xx" represents the mean size of the gold nanoparticles in nanometers. AuNP (20 nm) decorated with PEG5k is denoted as Au20PEG5k.

The size ($2R_h$) and zeta-potential of AuNPs before and after decoration are shown in Fig. 1. Two different citrate-stabilized AuNPs with nominal mean size of 20 and 10 nm were used. The DLS measurements give sizes ($2R_h$) of 21.6 nm and 10.1 nm, respectively (Fig. 1a). After decoration by OEG thiols, the values of mean size increase to $2R_h = 28.2 \pm 0.5$ nm and 15.7 ± 0.5 nm for Au20EG6OH and Au10EG6OMe, respectively. The increase of size is mainly due to the size of thiol molecules which is about 2.5 nm and overall the diameter increases by 5.0 nm [43]. Other effects, such as different hydration of the different end groups, only contribute minor changes on size measurements. PEG5k coated 20 nm AuNPs have a mean size of $2R_h = 43.8 \pm 0.5$ nm including the thickness of the PEG5k layer (~11 nm), which is consistent with the value reported in the literature [37].

The zeta potential measurements (Fig. 1b) shows a different scenario: while the zeta potential distribution of the 10 nm citrate stabilized AuNPs is relatively narrow and centered at -30.9 ± 5.0 mV, the 20 nm AuNPs show a broad distribution with a maximum at -33.9 ± 5.0 mV. After decoration, the zeta potential values are significantly reduced. For Au10EG6OMe and Au10EG6OH the zeta potential distribution curves are centered at -5.9 ± 5.0 mV and -15.1 ± 5.0 mV, respectively. In both cases, the zeta potential values are significantly smaller than the original citrate stabilized AuNPs. Au20EG6OH has a narrower distribution of zeta potential with a center of -18.0 ± 5.0 mV. For comparison, Au20PEG5k has weakly negative zeta potential of -9.0 ± 2.0 mV.

The long-term stability of Au20EG6OH solution (without added proteins) has been examined after storing in a refrigerator at 4 °C

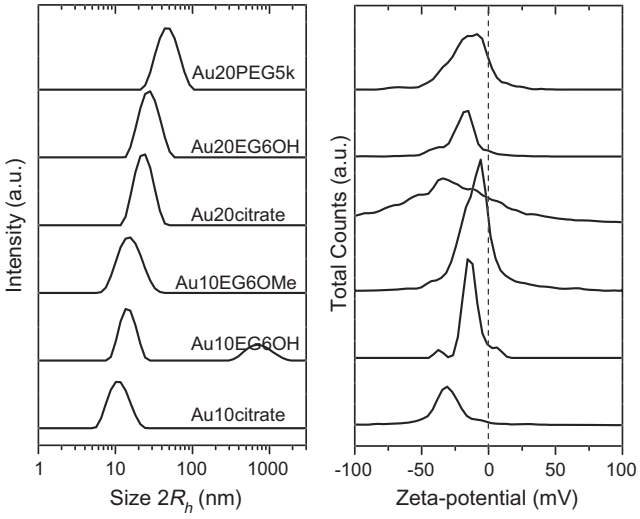

Fig. 1. (left) Size ($2R_h$) and (right) zeta potential measurements of 10 and 20 nm citrate stabilized AuNPs before and after decoration by OEG and PEG thiols. Decoration leads to a slight size increase with OEG, and a larger increase (~22 nm) by PEG5k. In both cases, the zeta potential values after decoration are significantly reduced. Plots are shifted vertically for clarity.

for 6 months, one and two years after sample preparation. The results of size and zeta potential measurements are shown in Fig. 2. For comparison, the results for the citrate stabilized 20 nm AuNPs and freshly prepared Au20EG6OH are also plotted in Fig. 2. In all cases, the DLS measurements give a similar size of 28.2 nm indicating no aggregation in the solution (Fig. 2a). Changes are observed from the zeta potential measurements (Fig. 2b): after 6 months storage at 4 °C, the zeta potential distribution remains almost the same compared to the fresh one, with the distribution centered at ~−15.1 ± 5.0 mV, but narrower. After one year, the distribution becomes broader; after two years storage, it becomes further broadened and two peaks are visible: the one with a small negative value is located in a similar position as the fresh colloids, while a more negative peak indicates the existence of highly charged colloids in the solution. Interestingly, in spite of the changes of the zeta potential, the colloidal solutions are still stable as no visible change on the size distribution could be seen. Stability tests with adding NaCl in the solution also support this conclusion; no visible change could be seen from the UV–visible spectra and visual inspection. The distribution of the zeta-potential is related to many factors in the system, such as the distribution of the charge state, the size distribution of the particles, dielectric constant of the solvent, and ionic strength. All these factors affect the mobility of the particles under the applied electric field, giving a distribution in the zeta-potential measurements. It is interesting to see that when the nanoparticles are nearly neutral, the zeta-potential distribution is very sharp (as one can see in Figs. 5a and b and 6) as all these effects are removed if the surface charge is neutralized.

To test the stability under extreme conditions, the colloid solution has been dialyzed against degassed milliQ water for 24 h. After dialysis, the mean size determined by DLS is still 28.2 nm, but the zeta potential becomes more negative and narrower with a center of −37.7 ± 5.0 mV. The changes in the zeta potential distribution may be due to the exchange of citrate molecules with thiols which leads to a broader distribution of the charge state of the nanoparticles. The colloid solution is stable and no visible change can be observed in the UV–visible spectrum. However, the colloidal solution is unstable by addition NaCl (data not shown), suggesting that the surface charge becomes the dominant stabilization effect and the nanoparticles behave as charge-stabilized colloids.

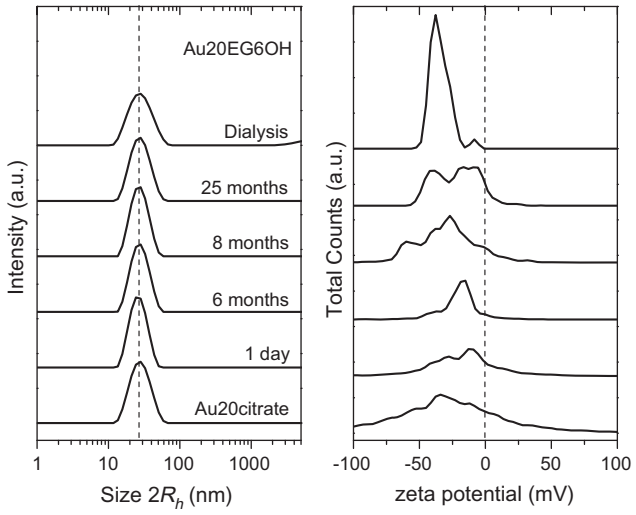

Fig. 2. Size (left) and zeta potential (right) measurements on Au20EG6OH after storage at 4 °C for various time up to 25 months suggest a long term stability of OEG coated AuNPs. There is no visible change on size, but zeta potential values shift slightly to more negative values. For comparison, the data for sample dialyzed against pure water is also shown, which is mainly stabilized by charge.

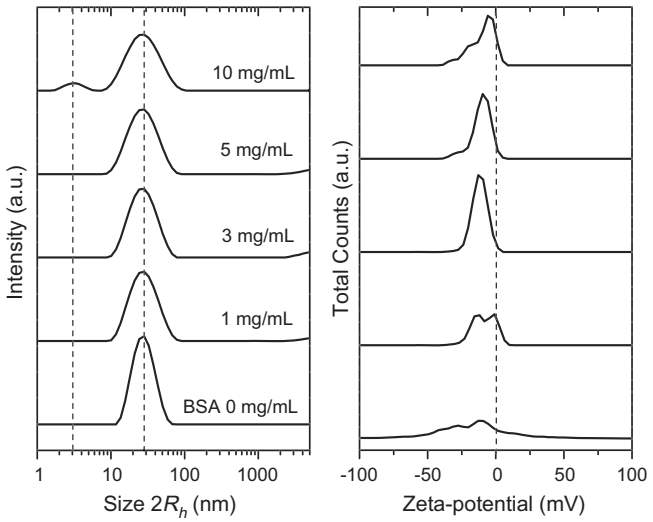

Fig. 3. Size and zeta potential measurements of Au20EG6OH with varying concentrations of BSA. There is no visible changes on size and the overall zeta potential values are negative for all samples tested in this work. The contribution from free BSA molecules starts visible for 10 mg/mL.

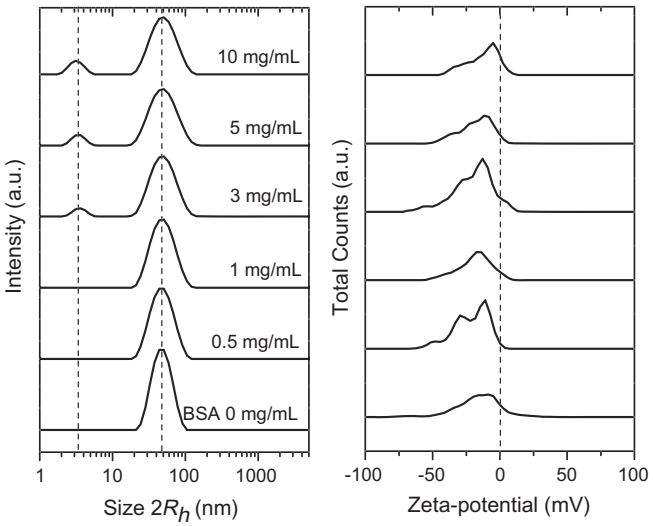

Fig. 4. Size and zeta-potential measurements of Au20PEG5k with varying concentrations of BSA. There is no visible changes on size and the overall zeta potential values are negative for all samples tested in this work. The contribution from free BSA molecules starts visible above 3 mg/mL.

3.2. Interactions of OEG and PEG SAM coated AuNP with proteins

Au20EG6OH is used as a model system to study the interactions with proteins in solution. Results from Au20PEG5k are also shown for comparison. Similar behavior and results of Au10EG6OMe can be found in supporting materials (Figs. S1 and S2).

3.2.1. Interaction with negatively charged proteins (BSA) at neutral pH

When protein (BSA) is added into the solution of Au20EG6OH, no visible change can be seen from the size measurements (Fig. 3), indicating neither significant aggregation nor protein adsorption. With 10 mg/mL BSA, an additional peak appears at an effective hydrodynamic diameter around 3 nm, which represents the faster collective diffusion of free BSA molecules [39]. Adding BSA leads to a narrowing of the distributions of zeta potential for the colloid, without significant change in the peak position. The

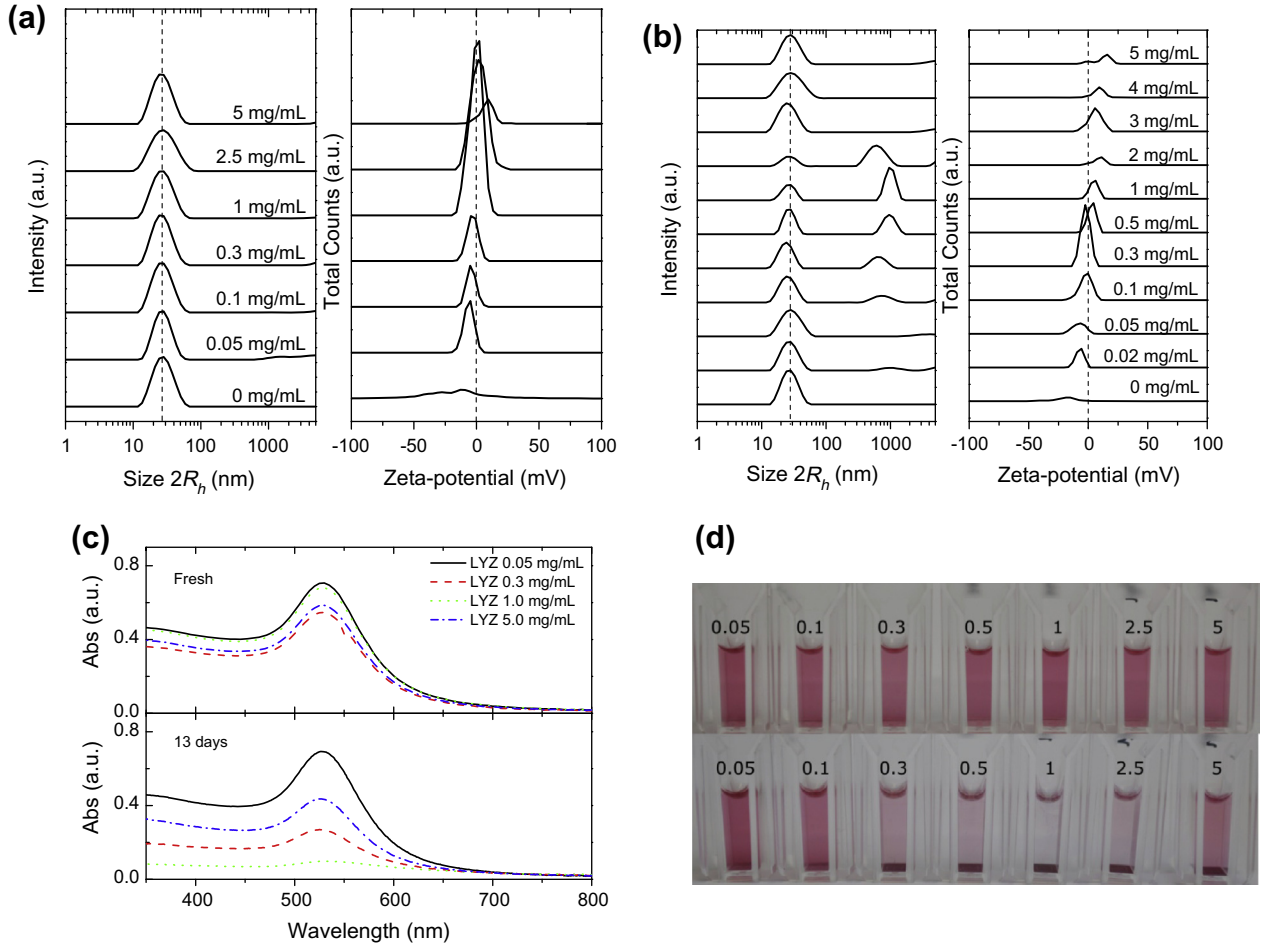

Fig. 5. (a and b) Size and zeta potential measurements of Au20EG6OH with varying concentrations of lysozyme (LYZ) in one week (a) and two weeks (b) after sample preparation. Short after sample mixing, no visible changes on size could be recognized, but zeta potential measurements indicate an effective charge inversion of the colloid, indicating the adsorption of lysozyme onto the colloidal surface. Two weeks after sample preparation, the size measurements show clearly an additional cluster peak for samples with zeta potential nearly zero. (c) UV–visible spectra of fresh and aged sample solutions; (d) photographs of sample solutions after preparation (top) and two weeks (bottom). (c and d) Further confirm the short-term stability of colloid-lysozyme mixtures.

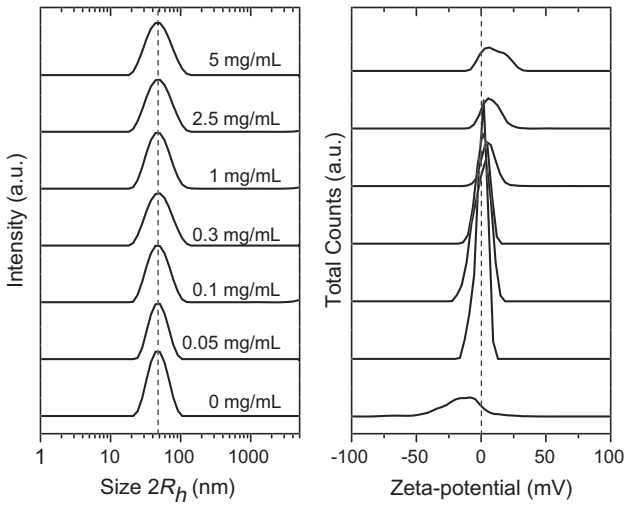

Fig. 6. Size and zeta-potential measurements of Au20PEG5k with varying concentrations of lysozyme. A similar charge inversion as in Fig. 5a with increasing protein concentration is observed. However, no visible size change could be recognized even after a month, indicating the long-term stability of PEG coated AuNPs.

overall charges are still negative and centered around −10 ± 5 mV. The experiments are repeated for freshly prepared sample solutions and also for samples after two weeks storage. No change could be observed in the size and zeta potential measurements.

Similar results are observed for Au20PEG5k solutions by addition of BSA (Fig. 4): No change is visible in the size measurements. Only the peak is slightly broadened. The additional peak appearing at ~3.4 nm above 3 mg/mL protein is due to the free proteins. In all cases the zeta potentials are negative without significant change. These results (Figs. 3 and 4) suggest that there is no aggregation of colloids and no detectable adsorption of protein to the colloid surface.

3.2.2. Interactions with positively charged protein (lysozyme) at neutral pH

When lysozyme is added into Au20EG6OH solutions, the stability of the mixture is found to be protein concentration dependent. A series of solutions with the same colloid concentration and increasing protein concentrations are prepared and measured immediately, one, two and four weeks after the sample preparation. Within the first week (Fig. 5a), the sample solutions are stable: there is only a single peak with mean size of 28.2 nm, corresponding to the colloid monomer and no clusters are visible in all DLS measurements. However, the corresponding zeta potential measurements show an interesting transition from negative to positive values with increasing the protein concentration. With 1 mg/mL lysozyme, the colloids are nearly neutralized. Further

increasing the protein concentration up to 5 mg/mL, the zeta potential becomes positive. Note here that for all the experiments, the pH of the solutions is in the range of 6.5–6.8, hence the pH effect on the surface charges can be neglected.

After two weeks, precipitates are observed for solutions with 0.3 up to 2.5 mg/mL lysozyme (Fig. 5d). However, the precipitates can be re-dispersed after shaking. The size measurements (Fig. 5b) after shaking show that the colloid monomer peak remains at the same position with increasing protein concentration, but a cluster peak corresponding to a size of a few hundred nanometers appeared for samples with 0.1–2 mg/mL lysozyme. The intensity of the cluster peak increases first with protein concentration, then decreases above 1 mg/mL of protein and the size of clusters is also smaller. Above 3 mg/mL, no cluster peak is visible. UV–visible measurements (Fig. 5c) before shaking show that the absorption intensity around the plasma peak (525 nm) is significantly reduced, in consistent with the precipitation of larger clusters. The corresponding zeta-potential values also show a continuous increase with protein concentration from negative to positive. After four weeks, the size measurements after shaking show much larger clusters and the precipitates become difficult to re-disperse (Supporting materials Fig. S3). Similar results are observed for EG6OMe decorated AuNPs (Au10EG6OMe and Au20EG6OMe with lysozyme, part of results are shown in supporting materials (Figs. S1 and S2).

The results of Au20PEG5k with lysozyme addition are presented in Fig. 6. The size of colloid remains at 43.8 nm with increasing protein concentration. Up to and including 5 mg/mL lysozyme, the signal of protein is not detectable. The lack of a significant signal is mainly due to the weak scattering of small lysozyme compared to the large colloid. The zeta potential measurements present a similar transition from negative to positive values with increasing protein concentration (Fig. 5a and b). No visible changes on size could be recognized even after a month, indicating the long-term stability of the PEG5k coated AuNPs.

3.2.3. Stability of the attached lysozyme to the colloid surface

A "washing" procedure (see experimental section) has been employed in order to check the stability of the lysozyme attached to the colloidal surface. Note that in general centrifugation is not a suitable way to concentrate or purify the OEG thiol coated AuNPs, since it leads to irreversible aggregation. However, after protein adsorption this becomes a convenient way for separation. The stability of the colloid after centrifugation and re-dispersion indicates the adsorption of lysozyme. Otherwise the aggregate after centrifugation cannot be re-dispersed as described in the experimental section. Using the sample solution of Au20EG6OH with 5 mg/mL lysozyme (one day after mixing) as the first example, we determine the zeta potential of the resulting colloidal solution after each round of centrifugation and re-dispersion (Fig. 7 left). After one round of washing, the zeta potential is reduced but still positive. After 4 or 5 washing rounds, the peak positions become negative, with -2.4 ± 2.0 mV and -5.2 ± 2.0 mV for 4 and 5 washing rounds, respectively. These values, however, are still higher than the sample without protein (-15.1 ± 5.0 mV in Fig. 1), but similar to that of the mixture with 0.05 mg/mL lysozyme (-5.4 ± 2.0 mV). These results suggest that some of proteins strongly adsorb to the colloid surface and cannot be washed away. If proteins were washed away completely, no re-dispersion would be seen.

Aging has a crucial impact on the adsorption of protein. For example, if the samples are stored more than 3 days after mixing, the washing experiments do not work anymore. The colloid aggregates after the first round of centrifugation cannot be re-dispersed. This may be due to the strong binding between protein and interface *via* the hydrophobic interactions [44].

For comparison, a mixture of Au20PEG5k with 5 mg/mL lysozyme is also washed following the same procedure (Fig. 7 right).

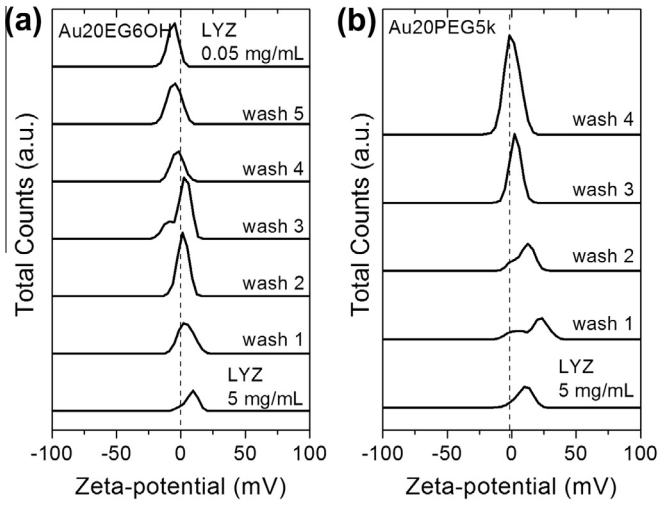

Fig. 7. Zeta-potential measurements of colloid-protein mixtures after several rounds of washing by centrifugation. (a) Au20EG6OH with lysozyme and (b) Au20PEG5k with lysozyme. In both cases, the zeta potential values decreases after washing, but do not go back to the original state. These results suggest that some of lysozyme molecules can tightly adsorb to the colloid surface and cannot be washed away.

After 4 rounds of washing the zeta potential becomes near neutral, further washing does not change the results significantly. During the washing procedure, the colloid solutions are always stable and easy to re-disperse. This can be explained by the steric effect of the long polymer chain [6,7].

3.3. Discussion

The observed surface charge on the OEG coated AuNPs and their interactions with proteins provide important information on understanding the protein non-fouling property at interfaces. Here we discuss the main observations and implications in the context of recent literature.

Firstly, these observations confirm the weak charge of OEG SAM on gold surfaces. Many studies exploring the protein-resistant mechanism of OEG SAMs on flat gold surfaces indicate that water penetration and hydroxide adsorption can cause a negative charge on the SAM surface, leading to a strong repulsive force between proteins and the interface [10,21,23,45]. Although the SAM on the surface of AuNP is not necessarily the same as that on the flat gold surface, the results presented in this work suggest two possibilities for the origin of surface charges: One is the adsorption of OH^-, in which the charges are located at the SAM–water interface. In the case of PEG, hydroxide ions can penetrate into the polymer brushes. The other way is the substitution of thiol molecules by free citrate molecules during aging or dialysis. In this case, the charges are located on the AuNP surface. Due to the facet nature of AuNP surfaces [1], the domain boundaries can cause defects in the SAM, i.e. the thiol molecules in these places have fewer neighboring molecules, which makes them less stable as they have a higher chemical potential. During a long-term storage or dialysis, these thiol molecules can detach and be substituted by citrates. Under these experimental conditions, the existence of the excess thiol molecules in colloid solutions seems important for their stability.

Secondly, at a flat interface, it has been shown that both OEG and PEG coated surfaces exhibit very good protein resistance property [46,47]. It is also known that the protein resistance property of OEG SAMs is highly dependent of the packing density and coverage. However, the coating process for colloids is quite different

from that on flat surfaces due to curvature, faceting and the fact that the colloids are pre-coated with citrate residues. We did not attempt to demonstrate if the nanoparticles are fully covered by the SAM. However, under the same conditions, we have used more thiols than needed for full coverage and the solutions were incubated over night to produce similar and high coverage. Compared to these studies at flat interfaces, the scenario of AuNPs is different. We do observe adsorption of proteins (lysozyme) to the weakly negatively charged functionalized AuNPs. It is therefore worthwhile to discuss the possible mechanisms of protein adsorption for OEG and PEG coated AuNPs.

It has been shown that BSA, despite the negative charge at neutral pH, adsorb to negatively charge surfaces, such as citrate-stabilized AuNPs and gold surfaces [48–50]. Protein adsorption of BSA is still possible even if protein and interface bear opposite global charges. Adsorption occurs through oppositely charged patches on protein and surface. In addition, adsorption at interfaces seems correlated to the secondary and tertiary structure stability of proteins [49]. Adsorption can occur also simply due to the electrostatic interaction, such as lysozyme adsorption to AuNP or silica surface in a large pH range, where lysozyme molecules are positively charged and AuNPs or silica particles are negatively charged [51,52]. While the flat OEG coated surfaces show good protein resistance property, the highly curved interface of nanoparticles can be different. Recently, curvature effect on the dissociation of ionizable ligands immobilized on nanoparticles has been rationalized by a theoretical model [36]. In our case, it is plausible that the high curvature of nanoparticles leads to a higher defect density and less ordered conformation of the OEG thiol molecules compared to flat SAM coated surfaces. These defects together with weak negative charge and van der Waals attraction can cause the adsorption or lysozyme.

Protein adsorption to PEG coated AuNPs can occur via different mechanisms. For polyelectrolyte grafted colloidal surface, it has been shown that negatively charged proteins (BLG, HSA, BSA) can adsorb to polyanionic brushes [53,54]. The protein adsorption at overall electrostatic repulsive surface can be explained by two possible mechanisms: first, charge regulation or reversal on protein surfaces due to the local electrostatic potential inside the polyelectrolyte brush [55]. Second, the entropically favorable replacement of small counterions inside the brush by protein molecules due to the charge anisotropy (patchiness) of the protein [54]. It has been demonstrated that the adsorbed proteins in the inner layer of the grafted polyelectrolyte brush are firmly bound and proteins in the outer layers are only weakly bound and can be washed out by ultrafiltration. However, these observations and the mechanism of protein adsorption may not be applicable to our system as PEG is intrinsically neutral. Even with the weak net charges discussed above, the charge density is not comparable with that of polyelectrolyte brushes. The major factor could be the interaction of the preferred binding sites on the surface of lysozyme with PEG. Furness et al. have identified the binding sites using proton nuclear magnetic resonance spectroscopy [56]. The residues of Trp-62, Arg-61 and Arg-73 in lysozyme have preferred hydrophobic interaction with the ethylene moieties.

It is interesting to see that on both OEG and PEG coated AuNPs, the adsorption of lysozyme leads to the effective charge inversion of the colloids. In the case of OEG coated AuNPs, this charge inversion affects the stability of the system (Fig. 5). Studies by Wang et al. have shown that mixing of lysozyme with charge-stabilized AuNPs at physiological pH leads to two types of aggregates: protein–AuNP assemblies and amorphous protein aggregates [51]. Recently, studies on the aggregation of silica nanoparticles with lysozyme have shown a different stability [52]. It was found that at pH 4-6, the aggregates are more compact. With increasing pH (7-9), the aggregates become a loose flocculated network. Further increasing the pH near the isoelectric point of lysozyme, the size of aggregates decreases dramatically. The mechanism of this unusual stability is due to the high negative charge of silica nanoparticles. When increasing pH, while the net positive charge of lysozyme decreases, the negative charge of silica nanoparticles increases, which reduces the attractive force via protein bridging [52]. In our system, the pH is nearly constant (6.8–7), the effective net charge, although weak, has a crucial effect on the stability of the OEG coated AuNPs. Minor adsorption of lysozyme neutralizes the surface charge and leads to the aggregation of colloids.

Finally, one should distinguish the different mechanisms of the colloid aggregation in the current study from our previous studies [31,33,34]. In the current study, colloid aggregation is mediated by the adsorbed proteins (lysozyme) at very low concentrations (<10 mg/mL) due to neutralization of the surface charge. In our previous work, adding proteins, mainly BSA (>100 mg/mL), into OEG coated AuNP solutions leads to a depletion-attraction between the larger colloids, which is an entropic effect, causing colloid aggregation [31,33,34]. Our further studies using other net-negatively charged proteins, such as ovalbumin, gamma-globulin, and bovine beta-lactoglobulin show similar results, i.e. colloid aggregation is observed above a critical protein concentration. However, adding lysozyme up to 250 mg/mL the colloid protein mixture is still stable (data not shown). It becomes clear now that the adsorption of lysozyme enhances the stability of the colloid, which is apparently due to the net-positive charge of lysozyme.

4. Conclusions

In this work, we have studied the size and surface charge of OEG or PEG coated AuNPs and their interactions with proteins in solution. We find that OEG and PEG coated AuNPs in aqueous solution present weak negative zeta potentials, indicating a weak negative charge. The OEG SAM on the colloid surface can be destroyed by long-term aging or dialysis, which finally renders the colloid non-resistant against non-specific protein adsorption. While BSA molecules with negative net charge do not adsorb or bind to these weakly charged colloids, lysozyme with positive net charge adsorbs to the surface of OEG/PEG coated colloids. The adsorption neutralizes the surface charge and leads to the aggregation of OEG coated AuNPs. The stability of PEG5k coated AuNPs is greater in the presence of lysozyme due to the entropic steric effect of the long polymer chain.

Acknowledgments

We gratefully acknowledge financial support from the Deutsche Forschungsgemeinschaft (DFG). F.R.-R. thanks the Studienstiftung des Deutschen Volkes for a fellowship.

Appendix A. Supplementary material

Supplementary data associated with this article can be found, in the online version, at http://dx.doi.org/10.1016/j.jcis.2014.03.052.

References

[1] J.C. Love, L.A. Estroff, J.K. Kriebel, R.G. Nuzzo, G.M. Whitesides, Chem. Rev. 105 (2005) 1103–1169.
[2] F. Schreiber, Prog. Surf. Sci. 65 (5–8) (2000) 151–257.
[3] F. Schreiber, J. Phys.: Condens. Matter. 16 (28) (2004) R881–R900.
[4] A. Ulman, Chem. Rev. 96 (4) (1996) 1533–1554.
[5] S. Schilp, A. Rosenhahn, M.E. Pettitt, J. Bowen, M.E. Callow, J.A. Callow, M. Grunze, Langmuir 25 (2009) 10077–10082.
[6] P.G. De Gennes, Macromolecules 14 (6) (1981) 1637–1644.
[7] S.I. Jeon, J.H. Lee, J.D. Andrade, P.G. De Gennes, J. Colloid Interface Sci. 142 (2) (1991) 149–158.

[8] L. Dressen, C. Humpert, P. Hollander, A.A. Mani, K. Ataka, P.A. Thiru, A. Peremans, Chem. Phys. Lett. 333 (5) (2001) 327–331.
[9] J. Zheng, L. Li, S. Chen, S. Jiang, Langmuir 20 (20) (2004) 8931–8938.
[10] J. Zheng, L. Li, H.K. Tsao, Y. Sheng, S. Chen, S. Jiang, Biophys. J. 89 (2005) 158–166.
[11] M.W.A. Skoda, R.M.J. Jacobs, J. Willis, F. Schreiber, Langmuir 23 (2007) 970–974.
[12] M.W.A. Skoda, F. Schreiber, R.M.J. Jacobs, J.R.P. Webster, M. Wolff, R. Dahint, D. Schwendel, M. Grunze, Langmuir 25 (7) (2009) 4056–4064.
[13] S. Zorn, N. Martin, A. Gerlach, F. Schreiber, Phys. Chem. Chem. Phys. 12 (31) (2010) 8985–8990.
[14] S. Zorn, M.W.A. Skoda, A. Gerlach, R.M.J. Jacobs, F. Schreiber, Langmuir 27 (6) (2011) 2237–2243.
[15] S. Zorn, U. Dettinger, M.W.A. Skoda, R.M.J. Jacobs, H. Peisert, A. Gerlach, T. Chassé, F. Schreiber, Appl. Surf. Sci. 258 (20) (2012) 7882–7888.
[16] K. Feldman, G. Hähner, N.D. Spencer, P. Harder, M. Grunze, J. Am. Chem. Soc. 121 (1999) 10134–10141.
[17] M. Zolk, F. Eisert, J. Pipper, S. Herrwerth, W. Eck, M. Buck, M. Grunze, Langmuir 16 (14) (2000) 5849–5852.
[18] S. Balamurugan, L.K. Ista, J. Yan, G.P. López, J. Fick, M. Himmelhaus, M. Grunze, J. Am. Chem. Soc. 127 (2005) 14548–14549.
[19] C. Dicke, G. Hähner, J. Am. Chem. Soc. 124 (2002) 12619–12625.
[20] S. Herrwerth, W. Eck, S. Reinhardt, M. Grunze, J. Am. Chem. Soc. 125 (2003) 9359–9366.
[21] H.J. Kreuzer, R.L.C. Wang, M. Grunze, J. Am. Chem. Soc. 125 (2003) 8384–8389.
[22] L. Li, S. Chen, J. Zheng, B.D. Ratner, S. Jiang, J. Phys. Chem. B 109 (2005) 2934–2941.
[23] A.J. Pertsin, T. Hayashi, M. Grunze, J. Phys. Chem. B 106 (2002) 12274–12281.
[24] M. Zheng, Z. Li, X. Huang, Langmuir 20 (10) (2004) 4226–4235.
[25] M. Zheng, F. Davidson, X. Huang, J. Am. Chem. Soc. 125 (2003) 7790–7791.
[26] M. Zheng, X. Huang, J. Am. Chem. Soc. 126 (38) (2004) 12047–12054.
[27] A. Aguila, R.W. Murray, Langmuir 16 (14) (2000) 5949–5954.
[28] K. Aslan, V.H. Pérez-Luna, Langmuir 18 (2002) 6059–6065.
[29] Y.-S. Shon, C. Mazzitelli, R.W. Murray, Langmuir 17 (25) (2001) 7735–7741.
[30] A.C. Templeton, J.J. Pietron, R.W. Murray, P. Mulvaney, J. Phys. Chem. B 104 (3) (1999) 564–570.
[31] F. Zhang, M.W.A. Skoda, R.M.J. Jacobs, S. Zorn, R.A. Martin, C.M. Martin, G.F. Clark, G. Goerigk, F. Schreiber, J. Phys. Chem. A 111 (2007) 12229–12237.
[32] J.N. Israelachvili, Intermolecular and Surface Forces, Academic Press Inc. (London) Ltd., London, 1985.
[33] F. Zhang, D.G. Dressen, M.W.A. Skoda, R.M.J. Jacobs, S. Zorn, R.A. Martin, C.M. Martin, G.F. Clark, F. Schreiber, Eur. Biophys. J. 37 (2008) 551–561.
[34] F. Zhang, M.W.A. Skoda, R.M.J. Jacobs, D.G. Dressen, R.A. Martin, C.M. Martin, G.F. Clark, T. Lamkemeyer, F. Schreiber, J. Phys. Chem. C 113 (2009) 4839–4847.
[35] K.P. Browne, B.A. Grzybowski, Langmuir 27 (4) (2010) 1246–1250.
[36] D. Wang, R.J. Nap, I. Lagzi, B. Kowalczyk, S. Han, B.A. Grzybowski, I. Szleifer, J. Am. Chem. Soc. 133 (7) (2011) 2192–2197.
[37] G. Zhang, Z. Yang, W. Lu, R. Zhang, Q. Huang, M. Tian, L. Li, D. Liang, C. Li, Biomaterials 30 (2009) 1928–1936.
[38] D.E. Koppel, J. Chem. Phys. 57 (4814) (1972).
[39] M. Heinen, F. Zanini, F. Roosen-Runge, D. Fedunová, F. Zhang, M. Hennig, T. Seydel, R. Schweins, M. Sztucki, M. Antalík, F. Schreiber, G. Nägele, Soft Matter. 8 (5) (2012) 1404–1419.
[40] A.V. Delgado, F. González-Caballero, R.J. Hunter, L.K. Koopal, J. Lyklema, J. Colloid Interface Sci. 309 (2) (2007) 194–224.
[41] M.D. Butterworth, R. Corradi, J. Johal, S.F. Lascelles, S. Maeda, S.P. Armes, J. Colloid Interface Sci. 174 (2) (1995) 510–517.
[42] J. López-Viota, S. Mandal, A.V. Delgado, J.L. Toca-Herrera, M. Möller, F. Zanuttin, M. Balestrino, S. Krol, J. Colloid Interface Sci. 332 (1) (2009) 215–223.
[43] D. Schwendel, T. Hayashi, R. Dahint, A. Pertsin, M. Grunze, R. Steitz, F. Schreiber, Langmuir 19 (2003) 2284–2293.
[44] P. Roach, D. Farrar, C.C. Perry, J. Am. Chem. Soc. 127 (22) (2005) 8168–8173.
[45] A.J. Pertsin, M. Grunze, Langmuir 16 (2000) 8829–8841.
[46] K.L. Prime, G.M. Whitesides, Science 252 (1991) 1164–1167.
[47] P. Harder, M. Grunze, R. Dahint, G.M. Whitesides, P.E. Laibinis, J. Phys. Chem. B 102 (1998) 426–436.
[48] H. Xie, A.G. Tkachenko, W.R. Glomm, J.A. Ryan, M.K. Brennaman, J.M. Papanikolas, S. Franzen, D.L. Feldheim, Anal. Chem. 75 (2003) 5797–5805.
[49] W.R. Glomm, Ø. Halskau, A.-M.D. Hanneseth, S. Volden, J. Phys. Chem. B 111 (51) (2007) 14329–14345.
[50] S.H. Brewer, W.R. Glomm, M.C. Johnson, M.K. Knag, S. Franzen, Langmuir 21 (2005) 9303–9307.
[51] D. Zhang, O. Neumann, H. Wang, V.M. Yuwono, A. Barhoumi, M. Perham, J.D. Hartgerink, P. Wittung-Stafshede, N.J. Halas, Nano Lett. 9 (2) (2009) 666–671.
[52] B. Bharti, J. Meissner, G.H. Findenegg, Langmuir 27 (16) (2011) 9823–9833.
[53] E. Bittrich, K. Rodenhausen, K.-J. Eichhorn, T. Hofmann, M. Schubert, M. Stamm, P. Uhlmann, Biointerphases 5 (4) (2010) 159–167.
[54] K. Henzler, B. Haupt, K. Lauterbach, A. Wittemann, O. Borisov, M. Ballauff, J. Am. Chem. Soc. 132 (9) (2010) 3159–3163.
[55] W.M. de Vos, F.A.M. Leermakers, A. de Keizer, M.A. Cohen Stuart, J.M. Kleijn, Langmuir 26 (1) (2009) 249–259.
[56] E.L. Furness, A. Ross, T.P. Davis, G.C. King, Biomaterials 19 (1998) 1361–1369.